RESEARCH ARTICLE

Development and Characterization of Transdermal Patches Using Novel Thymoquinone-L-Arginine-Based Polyamide Nanocapsules for Potential Use in the Management of Psoriasis

Eman Zmaily Dahmash[1] · Lama Murad Attiany[2] · Dalia Ali[3] · Shereen M. Assaf[4] · Jamal Alkrad[2] · Hamad Alyami[5]

Abstract

Thymoquinone (TQ) is a phytochemical compound present in *Nigella sativa* and has potential benefits for treating dermatological conditions such as psoriasis. However, its clinical use is limited due to its restricted bioavailability, caused mainly by its low solubility and permeability. To overcome this, a new transdermal drug delivery system is required. Nanoparticles are known to enhance material solubility and permeability, and hence, this study aimed to synthesize TQ-loaded L-arginine-based polyamide (TQ/Arg PA) nanocapsules incorporated into transdermal patches for prolonged delivery of TQ. To achieve this, Eudragit E polymer, plasticizers, and aloe vera as penetration enhancer were used to develop the transdermal patch. Furthermore, novel TQ/Arg-PA was synthesized via interfacial polymerization, and the resultant nanocapsules (NCs) were incorporated into the matrix transdermal patch. The Arg-PA NCs' structure was confirmed via NMR and FTIR, and optimal TQ/Arg-PA NCs containing formulation showed high entrapment efficiency of TQ (99.60%). Molecular and thermal profiling of TQ/Arg-PA and the transdermal patch revealed the effective development of spherical NCs with an average particle size of 129.23 ± 18.22 nm. Using Franz diffusion cells and synthetic membrane (STRAT M®), the *in vitro* permeation profile of the prepared patches demonstrated an extended release of TQ over 24 h, with enhanced permeation by 42.64% when aloe vera was employed. In conclusion, the produced formulation has a potential substitute for corticosteroids and other drugs commonly used to treat psoriasis due to its effectiveness, safety, and lack of the side effects typically associated with other drugs.

Keywords L-arginine · nanocapsules · polyamide · psoriasis · thymoquinone · transdermal patch

Introduction

Psoriasis is a chronic inflammatory skin disorder that affects around 1–3% of the world's population. The primary goal of pharmacological management of psoriasis is to reduce the side effects that could hinder the patient's day-to-day activities, social life, or overall health, and ultimately enhance their quality of life [1]. Psoriasis triggers the skin to thicken due to excessive growth of epidermal cells, resulting in epidermal hyperproliferation. Additionally, it can cause changes in the microvasculature of the upper layer of the dermis, including elongation and dilation of skin capillaries [2].

Psoriasis patients can be treated in three ways—topical, systemic, and phototherapy, depending on the severity of the disease. However, there is currently no single effective treatment available to manage psoriasis for several reasons, including nonadherence to therapy, drug toxicity, and tolerability [3]. Therefore, other therapies could be explored

✉ Eman Zmaily Dahmash
  e.dahmash@kingston.ac.uk

1 Department of Chemical and Pharmaceutical Sciences, School of Life Sciences, Pharmacy and Chemistry, Kingston University, London KT1 2EE, UK

2 Department of Applied Pharmaceutical Sciences and Clinical Pharmacy, Faculty of Pharmacy, Isra University, Amman 11622, Jordan

3 Department of Physiotherapy, Faculty of Allied Medical Sciences, Isra University, Amman 11622, Jordan

4 Department of Pharmaceutical Technology, Faculty of Pharmacy, Jordan, University of Science and Technology, P. O. Box 3030, Irbid 22110, Jordan

5 Department of Pharmaceutics, College of Pharmacy, Najran University, Najran 55461, Saudi Arabia

to maximize the response [4]. Topical treatments, such as topical corticosteroids, are used to manage mild to moderate psoriasis [1]. However, the use of steroids is limited due to the occurrence of systemic or local side effects [5].

There are several natural compounds with potent bioactive properties that are known to have anti-psoriatic effects, such as curcumin, resveratrol, and thymoquinone. However, the clinical applications of these natural bioactive compounds are limited due to their poor water solubility and low skin permeability [6, 7]. Thymoquinone (TQ) is a phytochemical compound found in the seed oil of black cumin, *Nigella sativa*. It has been associated with several health benefits such as analgesic, anti-diabetic, anti-hypertensive, anti-oxidative, anti-inflammatory, anti-hyperlipidemic, anti-microbial, anti-cancer, and anti-psoriatic activity [8–13]. Furthermore, TQ has a high safety profile, even at a dose of 90 mg/kg [14]. TQ targets inflammatory cytokines, molecular signaling pathways, and oxidative agents, in addition to controlling inflammation, regulatory T cells, and epigenetic alterations. These characteristics make TQ a potential candidate for the treatment of autoimmune diseases such as psoriasis [5, 10]. However, the clinical application of TQ is limited due to its low bioavailability caused by its low solubility, permeability, and stability. Some studies have also shown that TQ had a slight irritant effects [15].

Aloe vera (AV) is a botanical ingredient that has shown promise in topical applications. It has been reported that the use of AV as a penetration enhancer can improve the permeability of poorly permeable actives, in addition to providing soothing, hydrating, and wound-healing benefits [16]. Moreover, AV has been found to suppress bacteria, fungi, and viruses; act as an anti-inflammatory agent; reduce pain and itching; and moisturize the skin [17–19]. Therefore, investigating the use of AV with TQ formulation could prove to be effective in enhancing the permeation for TQ and acting as a soothing agent.

Transdermal drug delivery system (TDDS) is a method of delivering an active pharmaceutical ingredient (API) through the skin over an extended period of time [20]. Compared to other routes of administration, like oral and parenteral, TDDS is more preferred as it promotes patient compliance and avoids first-pass metabolism. TDDS is designed using specific membranes that control the release rate of the API over an extended period, therefore reducing dosing frequency [20–24].

There are numerous types of polymeric nanocarriers, including nanocapsules [7, 11], nanoemulsions [25], oleoethosomes [26], liposomes [27], solid lipid nanoparticles [28], and niosomes [25], that have been shown to significantly enhance the bioavailability and bioactivity of TQ. When TQ is loaded into a nano-sized polymer, it is expected to improve many of its properties, such as poor skin penetration, low permeability, solubility, and stability [7]. For

instance, a recent study by Bruno *et al*. demonstrated that encapsulating TQ within oleoethosomes nanovescicles enhanced its photostability and anti-inflammatory activity [26]. Therefore, a well-formulated TQ product could potentially replace or become an adjuvant to corticosteroids or other topical drugs, as it is effective, safe, affordable, and free of the common side effects associated with steroids [15].

Polymers play a crucial role in controlled drug delivery, including nanoparticles. These polymers can either be natural or synthetic, biodegradable, or nonbiodegradable [29, 30]. Biodegradable synthetic polymers have several advantages over natural polymers, such as avoiding microbial contamination and batch-to-batch variability [31]. Biodegradable polymers made using amino acid are highly valued in biomedical applications. These polymers are made from natural amino acids, which are the building blocks of proteins. Therefore, they are considered biocompatible, biodegradable, and have a high metabolism rate for their products [32].

L-arginine is an amino acid that has been extensively researched for its multiple applications. Polymers based on L-arginine have been reported. For example, L-arginine poly(ester amide)s, which are biodegradable polymers, have gained particular relevance in the biomedical field due to their favorable mechanical and thermal properties, as well as low toxicity of their degraded by-products [7, 33, 34]. These polymers have been used as carriers to facilitate insulin transdermal delivery, improve medication diffusion and distribution via the skin [35], and successfully deliver high doses of TQ into the lungs using dry powder inhalers [7]. Additionally, L-arginine-based polyamide was used to encapsulate promethazine HCl and produce taste-masked nanoparticles [36], while unsaturated L-arginine-poly(ester amide)s in an aqueous solution were used to create cationic hydrogels [37]. In recent studies, L-arginine-based polymers were found to be effective in gene transportation, gene condensation, and release [38]. Scientists have also investigated the bioactivity of L-arginine and found that it has excellent biosafety, antibacterial capabilities, and positive impact on wound healing [39]. For these reasons, L-arginine was chosen as the amino acid of choice in this study.

Poly(amide) polymers can be synthesized using various methods. The most used method is ring-opening polymerization. Another method is solution polycondensation, where monomers are dissolved in a nonreactive solvent with a catalyst to produce a soluble polymer. Melted polycondensation is a solvent-free technique that does not require post-treatment after the polymerization reaction, making it ideal for industrial manufacturing. Interfacial polymerization is another approach, which involves a condensation reaction between two quickly reacting monomers dissolved in immiscible solvents. Water is usually the preferred immiscible solvent, comprising the first phase with diamine or

diol compounds as well as an inorganic base. The other phase includes dichloromethane, toluene, or hexane, along with diacid chloride. When the two solutions are mixed, the polymer forms at or around the liquid-liquid interface [40–42]. Interfacial polymerization is simple and widely used approach in many disciplines, such as pharmaceutical encapsulation of APIs and preparation of conductive polymers [43].

In this study, a novel drug delivery method was investigated to improve the permeability, solubility, and stability of TQ. Nanoparticles have proven effective in delivering different APIs due to their small size and unique surface characteristics. They can also enhance solubility, modify permeability, and improve pharmacokinetic effects while preventing degradation and retaining encapsulated molecules [11]. Therefore, the aim of this study was to use nanotechnology to design and evaluate transdermal patches that can provide sustained delivery of TQ. L-arginine-based polyamide nanocapsules (NCs) containing TQ were developed using interfacial polymerization and embedded in a bi-layer transdermal patch that contained aloe vera. The produced NCs and transdermal patches were characterized.

Materials and Methods

Materials

Thymoquinone powder was obtained from Biosynth Carbosynth Ltd. (Compton, UK), L-arginine was purchased from Acros Organics (Geel, Belgium), and glycerin was obtained from LabChem Inc. (NJ, USA). Eudragit E100 was obtained from Evonik GmbH (Krefeld, Germany). Ethylene vinyl acetate (EVA) was obtained from Polysciences, Inc. (Warrington, Pennsylvania, USA), and Span 60 (Sorbitan monostearate) $(C_{24}H_{46}O_6)$ was obtained from Hangzhou Soy MedTech Company Ltd. (Hangzhou, China). Sodium chloride (NaCl) and sodium hydroxide were purchased from Fisher Scientific (Hampton, NH, USA). Ethyl acetate $(C_4H_8O_2)$ was obtained from Carbon Group Company (London, UK). Acetonitrile for HPLC (CH_3CN) and 2-6-pyridine dicarboxylic acid chloride (2,6-pyridinedicarbonyl chloride) were obtained from Honeywell Specialty Chemicals (Seelze, Germany). Dichloromethane (CH_2Cl_2) was obtained from Carlo Erba Reagents Srl (Cornaredo, Italy). Dimethyl sulfoxide (DMSO) and dimethylformamide (DMF) were obtained from Acros Organics (Geel, Belgium). Chloroform $(CHCl_3)$, diethyl ether $(C_2H_5)_2O$, trifluoroacetic acid (TFA), and acetone (C_3H_6O) were obtained from Alpha Chemika (Mumbai, India). Methanol (CH_3OH), isopropyl alcohol (C_3H_8O), and HPLC-grade distilled (H_2O) were obtained from Tedia highpurity solvents (Fairfield, CT, USA). Ethanol was obtained from E&C Chemicals, Inc. (Carrollton, GA, USA). Aloe vera $(C_{16}H_{13}NO_3)$ was donated from Natural Glow Ltd. (Amman, Jordan). All chemicals were used as supplied.

Synthesis of Polyamide Based on Arginine (Arg-PA)

L-arginine amino acid (0.87 g, 5 mmol), sodium hydroxide (NaOH) (0.40 g, 10 mmol), and 1 g of sodium chloride (NaCl) were added in a round-bottomed flask and dissolved in 5 mL of distilled water. The solution was stirred at a temperature between 0 and 5 °C. In a separate flask, 1.00 g (5 mmol) of 2,6-pyridinedicarbonyl dichloride was dissolved in 5 mL chloroform. The resulting solution was then added dropwise to the aqueous solution with continuous stirring until a yellow polyamide precipitate was formed. The precipitate was filtered using suction filtration and washed three times with distilled water. It was then filtered again and dried in a freeze dryer (Virtis benchtop Pro with Omnitronics™ from SP Scientific (Warminster, PA, USA)) for 8 h to remove all residual solvents. The freeze-dried powder (Arg-PA) was stored at room temperature until used later for further analysis.

Synthesis of Polyamide Based on Arginine-Thymoquinone Nanocapsules (TQ/Arg-PA) NCs

L-arginine amino acid (0.87 g, 5 mmol) and sodium hydroxide (0.40 g, 10 mmol) were added to a round-bottomed flask with 1 g of NaCl and dissolved using 5 mL of distilled water. The solution was stirred at 0–5 °C. Then, 1 g (5 mmol) of 2,6-pyridinedicarbonyl dichloride and 0.5 g of thymoquinone were dissolved in 20 mL chloroform and added to the aqueous solution drop by drop with continuous stirring until the yellow thymoquinone-loaded polyamide (TQ/Arg-PA) precipitate was formed. The TQ/Arg-PA precipitate was filtered with suction filtration, then washed three times with distilled water, filtered again by suction filtration, and dried in a freeze dryer for 8 h to remove all residual solvents. The freeze-dried powder (TQ/Arg-PA) was stored at room temperature for further analysis.

Preparation of the Double-Layered Transdermal Patches

The transdermal patches consisted of two layers: the backing layer (EVA-based layer) and the medicated layer (made of an extended release matrix using Eudragit E100). To prepare the backing layer, a 3% (w/v) EVA solution was used. The solution was made by adding 3 g of EVA to 100 mL of dichloromethane and stirring on a magnetic hotplate (25 °C, 500 rpm) until fully dissolved. The resulting solution was then cast onto a glass Petri dish with a diameter of 8 cm (50.24 cm^2) in amounts

of 25.5 mL/dish (0.51 mL/cm^2). The layer was allowed to dry at room temperature for 2 days. The transdermal patches were prepared according to the method described in Assaf *et al.* [44].

The second layer of the transdermal patch was created using different concentrations of Eudragit E that were dissolved in a mixture of 40% acetone and 60% isopropyl alcohol. Glycerin was added as a plasticizer at varying concentrations (see Table I). Aloe vera was used as a penetration enhancer, and Span 60 was used as an emulsifier. The second layer was then poured over the dried EVA layer and left to dry. Table I provides a summary of the composition of all prepared formulations and their respective drying conditions.

Arg-PA and TQ/Arg-PA NC Characterization

Several profiling techniques were used to characterize the synthesized polyamide (Arg-PA) and the thymoquinone-polyamide (TQ/Arg-PA) NCs.

Solubility Test

To determine the solubility of (Arg-PA) and (TQ/Arg-PA) NCs, 10 mg of each was separately dissolved in 2 mL of ten different solvents including water, ethyl acetate, methanol, ethanol, chloroform, acetone, diethyl ether, DMSO, DMF, and acetonitrile at 25 °C. The solubility was evaluated visually, and the results were categorized as completely dissolved (+), partially dissolved (−/+), or not dissolved (−).

Fourier Transform Infrared (FTIR) Spectroscopy Analysis

The PerkinElmer FTIR spectrometer (OH, USA) was used to operate the FTIR spectra of TQ, Arg-PA, and TQ/Arg-PA NCs, with the assistance of Spectrum 10 software. A few milligrams of each sample was loaded onto a sample holder, placed above a laser lens, and held in place by screwing down the relevant adaptor. The FTIR spectrum scans of each sample were obtained over the range of 450–4000 cm^{-1} with a resolution of 2 cm^{-1}.

Nuclear Magnetic Resonance (NMR) Spectroscopy

The ^{1}H-NMR and ^{13}C-NMR spectra of the Arg-PA were recorded on a Bruker Avance 500 MHz spectrometer (Bruker DPX-500) using tetramethylsilane (TMS) as the internal standard.

Differential Scanning Calorimetry (DSC) Analysis

Using a DSC Q200-TA instrument (USA), Arg-PA and TQ/Arg-PA NCs were subjected to DSC analysis. A 3 mg sample was placed on an aluminum pan and heated at a rate of 10 °C/min while being continuously purged with nitrogen at a rate of 50 mL/min.

Particle Size Analysis, Polydispersity Index, Zeta Potential, and Transmission Electron Microscopy (TEM)

The average particle size, polydispersity index (PDI), and zeta potential of TQ, Arg-PA, and TQ/Arg-PA NCs were measured at 25 °C using a Zeta Sizer Nano ZS90 (Malvern Instrument, UK). Samples were diluted with deionized water and put through a 1-min sonication bath before analysis. The analysis was carried out three times. The results were

Table I Composition and Processing Conditions used in the Preparation of the Double-layered Transdermal Patch (Patch Area = 50.24 cm^2)

Patch no.	Backing layer (first)	Medicated layer (second layer)					Drying conditions
	EVA (mg)	Eudragit E100 (mg)	Glycerin (µL)	Aloe vera (µL)	Span 60 (mg)	TQ/Arg-PA (mg)	
P1	-	560	115	-	-	-	5 h 40 °C
P2	765	-	-	-	-	-	5 h 40 °C
P2	-	560	115	-	-	-	24 h RT
P3	765	560	115	-	-	-	24 h RT
P4	765	960	190		-	-	24 h RT
P5	765	1275	190		-	-	24 h RT
P6	765	1912	190		-	-	24 h RT
P7	765	1912	300	200	-	-	24 h RT
P8	765	560	300	100	150		24 h RT
P9	765	560	300	100	70	-	24 h RT
P10	765	560	300	100	70	500	24 h RT
P11	765	560	300		70	500	24 h RT

presented as mean and standard deviation (SD). The TEM analysis of (TQ/Arg-PA) NCs was tested using JSM-IT300 (JEOL, Japan).

X-ray Diffraction (XRD) Analysis

TQ, Arg-PA, and TQ/Arg-PA NC physical characteristics were investigated using X-ray diffractometry on a MiniFlex 600 benchtop diffractometer from Tokyo, Japan's Rigaku. The XRD studies used Cu K radiation (1.5148227 Å) over a range of 2θ from 5 to 99°, at a voltage of 40 kV and a current of 15 mA. Data was gathered at a 5°/min scanning rate. OriginPro® software was used to evaluate the scans (OriginLab Corporation, USA).

Quantification of TQ Using High-Performance Liquid Chromatography (HPLC)

Dionex Softron HPLC System from Thermo Fisher Scientific Inc. was used for the quantification of TQ. It included an ultraviolet (UV) detector set at 250 nm, and a Fortis-C18 (Fortis Technologies Ltd. C 18. 250 × 4.6 mm) analytical column. A mixture of acetonitrile (ACN) and 0.125% v/v trifluoracetic acid (TFA) water at a ratio of (80:20% v/v) constituted the mobile phase. The column temperature was set at 20 °C, the injection volume for the sample was 20 μL, and the flow rate was 1 mL/min. The HPLC method's validity, accuracy, precision, linearity, limits of detection (LODs), and limit of quantification (LOQ) were all confirmed in accordance with International Council for Harmonization (ICH) criteria [45]. A 100 mg of TQ was dissolved in 100 mL of ACN to prepare a stock solution which was further diluted to produce concentrations between 3.90 and 1000 μg/mL.

Entrapment and Loading Efficiencies

The entrapment efficiency (EE %) and loading efficiency (LE %) of TQ in the produced formulations were calculated using Eqs. (1) and (2), respectively.

$$EE\,(\%) = \frac{TQ_i - TQ_f}{TQ_i} \times 100 \tag{1}$$

$$LE\,(\%) = \frac{TQ_i - TQ_f}{(TQ/Arg - PA)_t} \times 100 \tag{2}$$

where TQ_i is the total initial amount of added TQ in the preparation of the nanoparticles, TQ_f is the amount of TQ not entrapped into the formula and removed in the filtrate, and $(TQ/Arg - PA)_t$ is the total amount of the produced formula after drying (yield). The filtrate was collected upon

the synthesis of the TQ-loaded NPs and utilized to perform HPLC-based analysis for TQ content..

Characterizations of the Transdermal Patch

The transdermal patches were characterized for their physical properties, drug content, and release studies. Measurements were done in triplicates and reported as mean ± standard deviation (SD).

Thickness and Weight Uniformity

Each patch's thickness was measured at five different points with a digital micrometer. A 1-cm^2 piece was cut from each patch and weighed using a digital scale to assess the weight uniformity. Results were reported as mean ± SD.

Drug Content

Three patches each measuring 1 cm^2 were cut-off. Then, each patch was added to a 50 mL solution of acetonitrile and stirred on magnetic stirrer until fully dissolved. The drug content was then assessed using HPLC after sample filtration using syringe filter with 0.45-μm aperture size.

Folding Endurance

The patch was folded repeatedly in the same location until it broke as a folding endurance test. The number of times it took to break the patch was recorded.

Solvent Residue

To determine the solvent residue in representative patches (P6, P8, P9, P10), 5 samples of each formula were placed in a desiccator with silica gel (0% relative humidity (RH)) at room temperature. The initial weight (W_1) of each patch was recorded before putting it in the desiccator (see Table IV). The weight of each patch was measured every 2 h until a stable value was obtained (W_2) and maintained for 4 h, as per Assaf *et al*. [44]. The difference between the initial and final weights of the patch (W_1 and W_2, respectively) in relation to its final weight was used to calculate the solvent residue (SR).

$$SR(\%) = \left(\frac{W1 - W2}{W2} \right) \times 100 \tag{3}$$

Moisture Uptake

To measure the moisture absorption of each patch using representative patches (P6, P8, P9, P10), 5 samples of each formula's initial weight (W_1) were recorded after 24 h of

storage at room temperature in a desiccator containing silica gel with 0% RH. The patches were then transferred to desiccators containing distilled water with 100% RH at room temperature and weighed every 2 h until a stable weight was achieved (W_2) and maintained for 4 h. The percentage of moisture absorption was calculated using the difference between the final weight (W_2) and the initial weight (W_1), in relation to the starting weight (Eq. 4).

$$\text{Moisture uptake (\%)} = \left(\frac{W_2 - W_1}{W_1} \right) \times 100 \qquad (4)$$

Stability of Transdermal Patches

Produced patches were stored in the refrigerator at 4 °C, ambient room temperature (~ 25 ± 2 °C), and oven at 40 °C (75% RH), for 3 months; the stability of the selected optimum patches was assessed. The patches were maintained in a closed container, covered in aluminum foil, and given a monthly visual inspection for physical appearance. The patches' physical characteristics and TQ content were evaluated after 3 months.

In Vitro Release and Permeation Studies

An *in vitro* release study of TQ from the transdermal patches was conducted using a 6-station Franz diffusion apparatus (Maharashtra, India) with a diffusion area of 4.91 cm^2 (25-mm-diameter orifice). Each receptor compartment had 20 mL of phosphate buffer (pH 6.8) at 32 ± 1 °C. The reported TQ aqueous solubility is 1–1.8 g/L [7, 46], and using 20 mL of buffer solution enabled the maintenance of sink conditions. The transdermal patch P10 or P11 (25-mm diameter) was installed between the donor and receptor compartments of the diffusion cell, with the backing layer facing the donor compartment. The receptor medium was stirred using magnetic stirrer. At regular intervals (0.5, 1, 2, 3, 4, 6, 12, 18, 24 h), 0.5 mL samples were collected through the sampling port from the receptor medium and promptly replaced with an equal volume of fresh buffer solution. The samples were stored at 25 °C in tightly covered amber HPLC vials until the drug content was determined by HPLC. The experiments were performed in triplicate, and the cumulative TQ release per cm^2 against time was obtained. Additional patches with a similar formulation to P10 were prepared but without aloe vera (P11) to compare the effect of aloe vera on the release and permeation behavior of TQ. The release profiles for the patches were fitted according to five mathematical models (zero order, first order, Higuchi, Hixon Crowell, and Korsmeyer-Peppas) [7, 47].

For the permeation study, a STRAT M® synthetic polymeric membrane (Merck, UK) was used to simulate the skin. The membrane was soaked in phosphate buffer for 24 h before use and placed between the donor and receptor compartments. To conduct the study, TQ-loaded transdermal patches (P10 and P11) were installed between the donor and synthetic membrane of a receptor compartment of the diffusion cell. The diffusion cell was firmly fastened in place with an O-ring. The same procedure for the release study was carried out. The steady-state flux (Jss) was calculated from the slope of the regression line, which represents the linear portion of the curve. The lag time was calculated from the intercept of the steady state line and the *x*-axis [44].

Statistical Analysis

The data was analyzed using Microsoft Excel software. Statistical analysis was performed using Minitab software version 21.10.1, with a significance level of 0.05. The analysis of variance (ANOVA) and a *t* test were conducted to compare the formulations. The results of the statistical analysis are presented as mean ± standard deviation (SD) for all formulations.

Results and Discussion

Synthesis of Arg-PA and TQ/Arg-PA NCs

In order to synthesize arginine-based polyamide (Arg-PA) and TQ/Arg-PA NCs, the interfacial polycondensation method was utilized. This involved dissolving the amino acid in the aqueous layer and pyridinedicarbonyl dichloride in the organic layer. At the interface between these two layers, the polyamide formation occurred, as illustrated in Fig. 1. The reaction required vigorous stirring to increase the surface area available for the reaction and to form fine particles.

Solubility Test

The solubility of the Arg-PA and TQ/Arg-PA NCs was assessed for the ability to dissolve in different solvents experimentally. The assessment was in the following solvents: water, ethyl acetate, methanol, ethanol, chloroform, acetone, diethyl ether, DMSO, DMF, and acetonitrile at 25 °C. The results demonstrated that the two materials were soluble in chloroform and acetone, slightly soluble in DMSO, DMF, and acetonitrile, while insoluble in water, ethyl acetate, ethanol, and diethyl ether.

FTIR Analysis

The FTIR spectra (Fig. 2) exhibited characteristic absorption bands for all organic functional groups of the TQ, Arg-PA, and TQ/Arg-PA NCs. The FTIR spectra of TQ (Fig. 2a)

Fig. 1 Synthesis process of polyamide based on L-arginine and pyridinedicarbonyl dichloride using interfacial polycondensation to form L-arginine polyamide (Arg-PA)
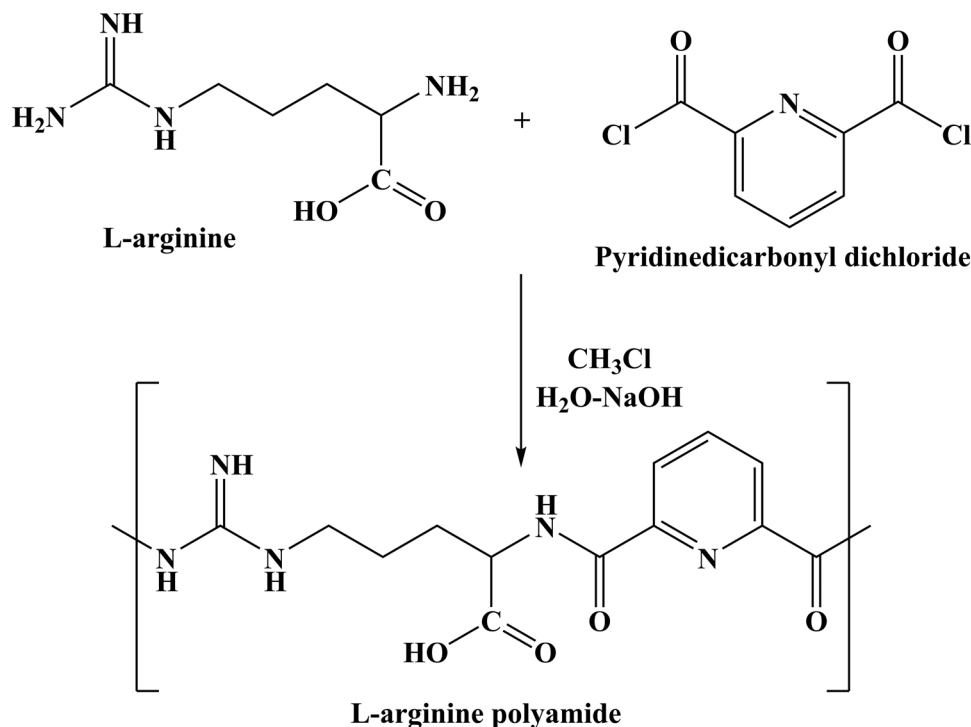
showed a characteristic band at 2915 cm^{-1} which represents the CH stretching. Additional band at 1718 cm^{-1} belongs to the C=O stretch of the ketone [48]. Arg-PA (Fig. 2b) and TQ/Arg-PA NCs (Fig. 2c) showed the same characteristic bands. The most important bands are the stretching vibration for the amide carbonyl group around 1640 cm^{-1}; this ensures the formation of the polymer. The CH-stretch band of TQ was still appearing in Fig. 2c; this may indicate the loading of TQ within the Arg-PA polymer.

NMR Spectral Analysis

Figure 3 presents the NMR analysis of ARG-PA. The samples showed characteristic chemical shifts in their spectra, which corresponded to the different atoms present. Please refer to Fig. 3a, b for details. The ^{1}H-NMR and ^{13}C-NMR chemical shifts for the various atoms have been summarized in Fig. 3c. The carbonyl carbon atoms in the Arg-PA are particularly important, as they highlight the formation of the polyamide. The carbon signals of the C=O groups of the formed amide groups were found to appear between 166.2 ppm, as shown in Fig. 3b.

Thermal Profile Analysis Using DSC

In Fig. 4, the results of the DSC analysis are presented. The thermogram of TQ in Fig. 4a indicates a sharp endothermic peak at 46.8 °C, which implies the melting point of TQ and confirms its crystalline nature. A shallow and broad peak at around 129.23 °C was represented, which could be either solvent residual or decomposition of the material, as reported by previous studies [7]. Figure 4b shows the thermogram of the L-arginine. It clearly displays an endothermic peak at 229.01 °C, which corresponds to the melting temperature of arginine and confirms its crystalline nature. However, the L-arginine-based polymerization produced amorphous ARG-PA-NCs, as demonstrated by Fig. 4c, which showed two broad and shallow peaks. The first one at 69.73 °C might represent the glass transition of the Arg-PA polymer. The second shallow broad peak at 120.39 could represent the evaporation of the residual solvent (water). Apparently, the polymer possesses an amorphous nature.

Finally, Fig. 4d presents the thermograms of a physical mixture made of the polymer (Arg-PA) and TQ blend (that is exactly similar to the content of the TQ-/Arg-PA NPs). The results show a sharp endothermic peak of the TQ melting process and a broad peak at around 179.31 °C. However, the TQ-loaded Arg-PA-NCs' thermogram in Fig. 4d did not reveal any endothermic peak of TQ while the shallow peaks of the glass transition and evaporation are still present. It is proposed that TQ may have transformed into an amorphous material, hence an improved solubility, or the drug is encapsulated within the polymer as reported by other researchers [36, 49].
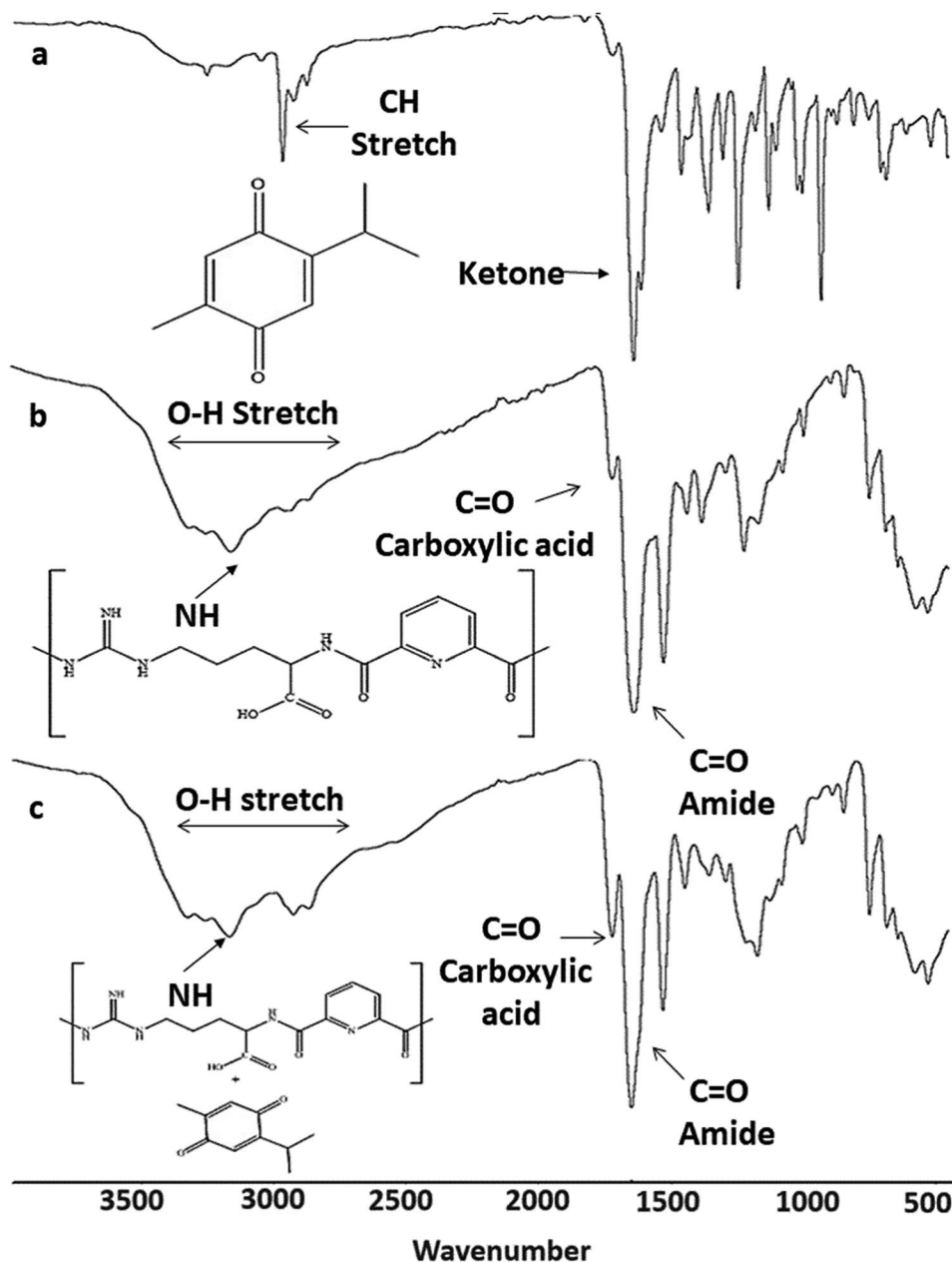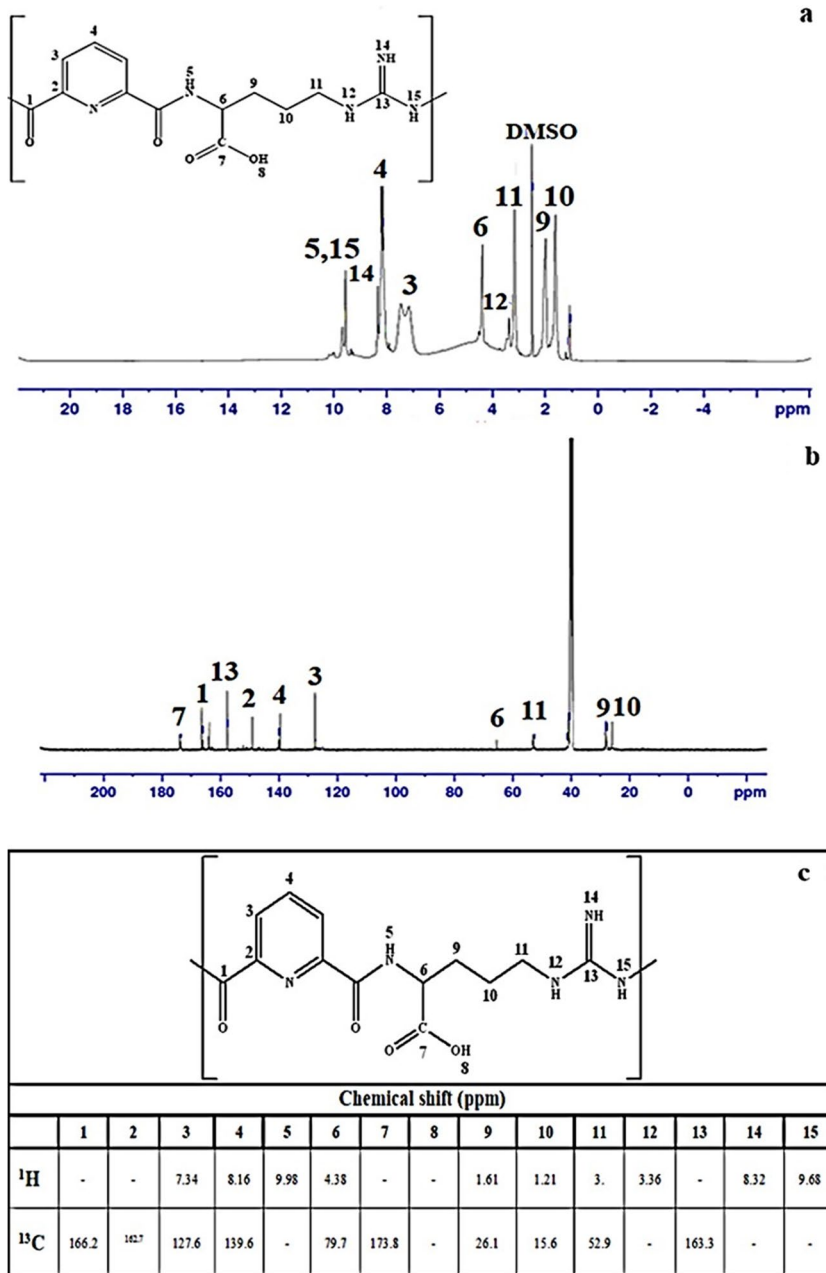
Particle Size Analysis, Zeta Potential, and TEM Analysis

Particle size analysis was conducted using a zeta sizer, and the findings are presented in Table II. TQ powder demonstrated nano-sized particles within the range of 390 ± 32.3 nm. However, after encapsulation and loading within the polymer using the interfacial polycondensation method, the final formula's size reduced to an average of 153 ± 13 nm. There was a slight but insignificant increase in the particle size after TQ was added to the polymer (t test $p > 0.05$), which was attributed to the encapsulation of TQ within the polymeric chains. Similar results were reported earlier [7,

49, 50]. According to the zeta potential, L-arginine had a positive charge, while TQ as a powder showed aggregated fine powder with a negative charge [51]. The formed polymer carried a positive charge which was attributed to the presence of L-arginine [52, 53]. The TQ/Arg-PA NCs again have a positive charge which is significantly less than that of the naked polymer due to the presence of TQ within it (t test, $p = 0.023$). However, the reduction in the surface charge resulted in a higher level of aggregation as can be seen from the PDI for the Arg-PA and the TQ/Arg-PA.

TEM images of TQ-loaded ARG-PA-NCs as can be seen in Fig. 5 revealed spherical NPs with sizes ranging from 80 to 180 nm. ImageJ software was used to calculate the

Fig. 3 NMR spectra of Arg-PA:
a ^{1}H NMR, **b** ^{13}C NMRm and **c**
chemical shift table

Chemical shift (ppm)															
	1	2	3	4	5	6	7	8	9	10	11	12	13	14	15
^{1}H	-	-	7.34	8.16	9.98	4.38	-	-	1.61	1.21	3.	3.36	-	8.32	9.68
^{13}C	166.2	162.7	127.6	139.6	-	79.7	173.8	-	26.1	15.6	52.9	-	163.3	-	-

average particle size, and it was 129.23 ± 18.22 nm. Such nanoscale particles will offer a significant surface area for the release of the encapsulated TQ and are advantageous for medication delivery. The zeta-sizer produced larger particles than what the TEM could produce. The high PDI and low charge indicate that the particles have aggregated, which may be the cause of this. However, because the polymer is biodegradable, it is anticipated that the polymer will progressively break down and release TQ upon application. It is worth mentioning that the particle size of the (TQ/Arg-PA) NCs using the zeta sizer was larger than that of the TEM which could also be attributed to the presence of a hydration layer around the particles in the zeta sizer technique [54].

XRD Analysis

XRD analysis of TQ as depicted in Fig. 6a showed a typical crystalline material with a sharp peak at 8.38° 2θ. Similar results were reported earlier [7]. L-arginine demonstrated crystalline nature with characteristic sharp peaks at 17.88°, 20.82°, 23.59°, 25.28°, and 26.78° 2θ (Fig. 6b). However, the polymer did not show characteristic sharp peaks, apart from two small peaks at 2θ 31.65° and 45.39° (Fig. 6c), and this follows the results obtained from the DSC analysis. The polymer is amorphous to semi-crystalline in nature. However, the TQ-loaded formula did not show any characteristic peaks for TQ (Fig. 6e), and this could be justified in two aspects. First,
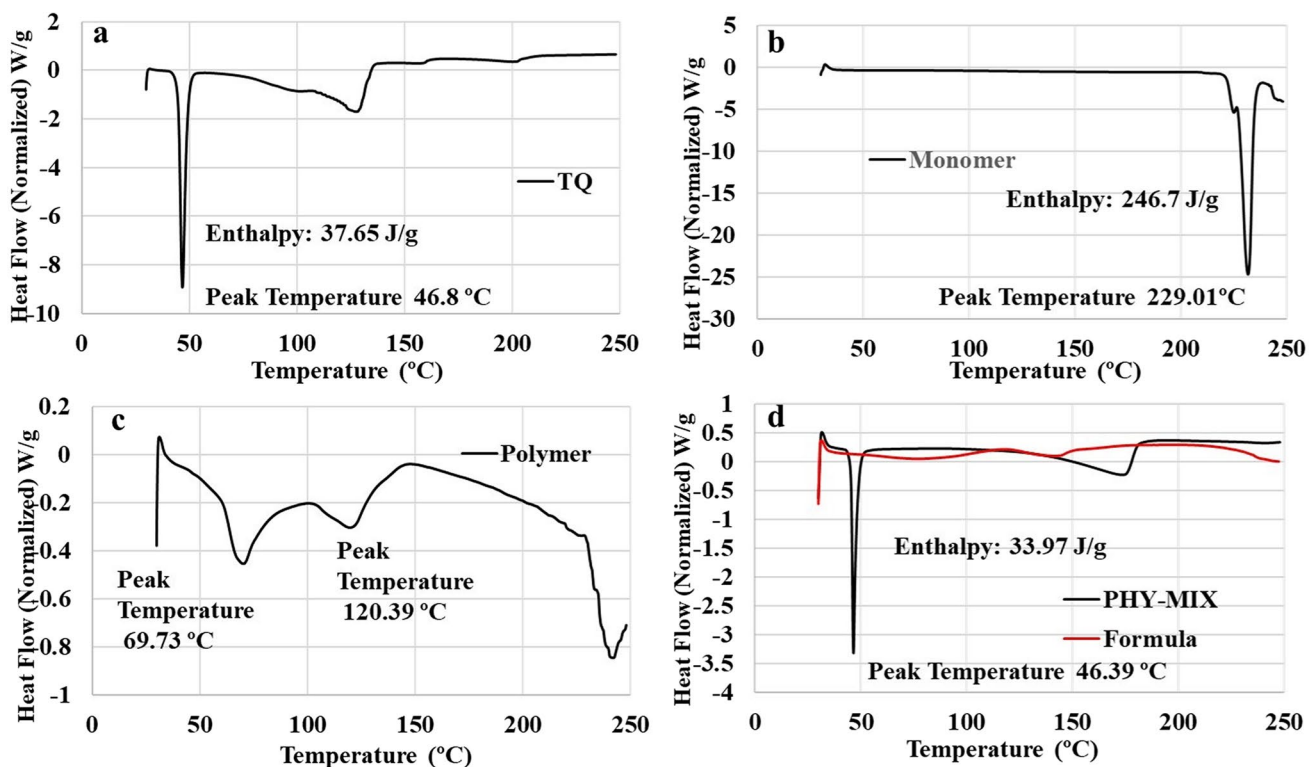
Fig. 4 DSC thermograms for **a** TQ powder, **b** L-arginine, **c** ARG-PA NCs, **d** the physical mixture (ARG-PA and TQ) as well as the TQ-loaded Arg-PA NCs

Table II Particle Size, PDI, and Zeta Potential for TQ, **L**-arginine, Arg-PA-NCs, and TQ/Arg-PA NCs (Mean ± SD, $n = 3$)

Parameter	Material			
	TQ	L-arginine	ARG-PA-NCs	TQ-ARG-PA NCs
PSA (nm)				
Mean ($n = 3$)	389.30	540.47	145.93	153.83
SD	32.3	215.6	21.6	13.0
PDI				
Mean ($n = 3$)	0.57	0.69	0.43	0.44
SD	0.09	0.09	0.13	0.02
Zeta potential (mV)				
Mean ($n = 3$)	− 47.13	+ 29.07	+ 33.27	+ 19.1
SD	1.22	2.10	1.37	0.56
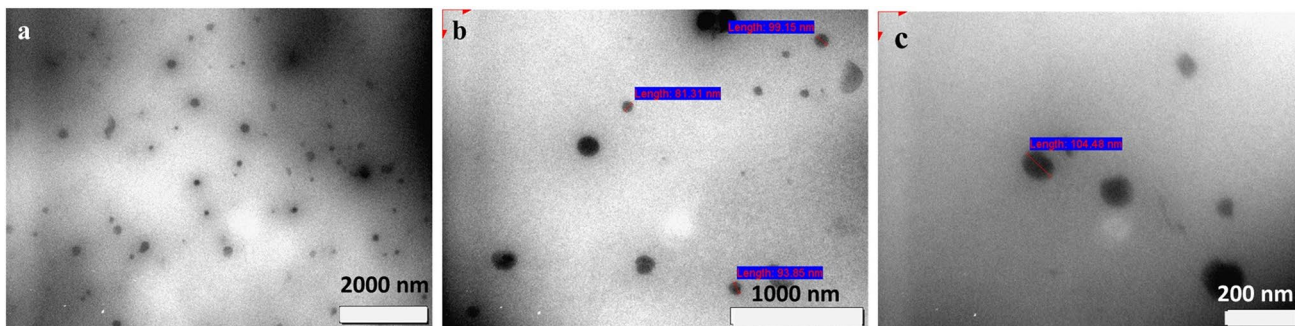
Fig. 5 TEM images of TQ-loaded L-ARG-PA NC scales: **a** 2000 nm, **b** 1000 nm, and **c** 200 nm
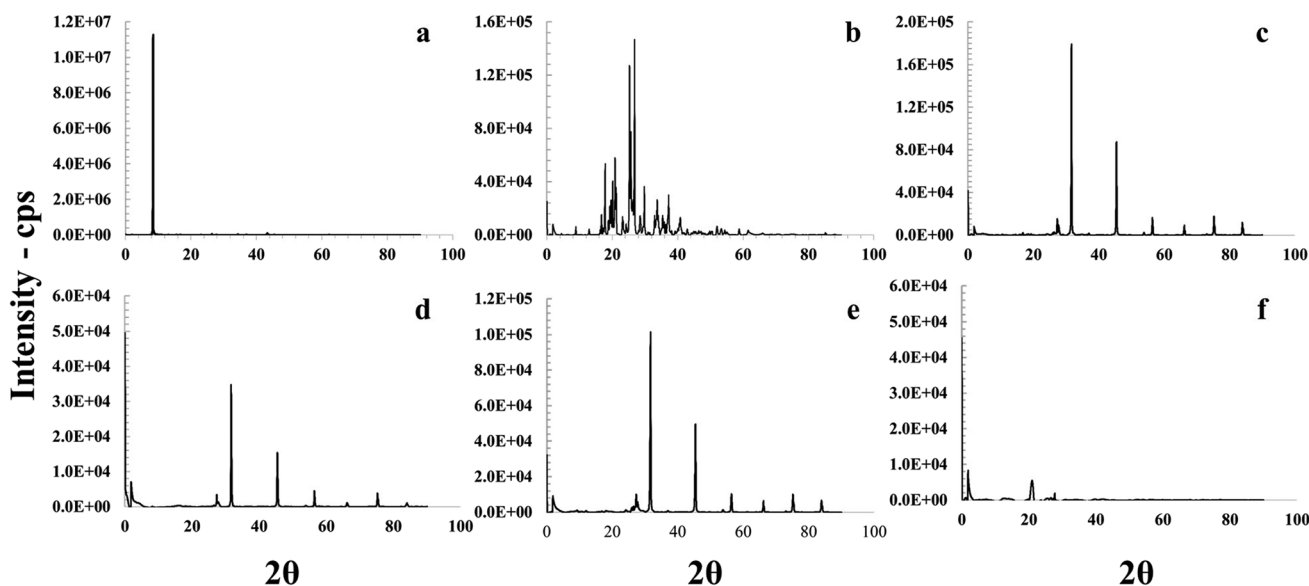
Fig. 6 XRD patterns for **a** TQ, **b** L-arginine, **c** ARG-PA NCs, **d** ARG-PA NCs + TQ physical mix, **e** TQ-loaded ARG-PA-NCs (formula), and **f** the blank film

TQ changed its nature from crystalline to amorphous, which is in concordance with the DSC results. Second, the inclusion or encapsulation within the polymer may result in the disappearance of the peak and that was reported in several studies [49]. The Arg-PA and TQ physical mixture showed results similar to the formula, and this could be attributed to the small quantity of TQ in the physical mix. The blank film (Fig. 6f) showed amorphous nature with no high intensity peaks.

HPLC Analysis

HPLC was employed for TQ quantification and was validated according to the ICH guidelines [45]. TQ demonstrated a retention time of 6.257 ± 0.056 min, while the solvent front was eluted at 2.031 ± 0.062 min. The method showed linearity within a concentration range of 3.9 to 62.5 µg/mL that produced a regression equation of $y = 1.2798x - 2.647$ (R^2 0.9996). The method was specific to TQ where solution of

Arg-PA, and other components of the transdermal patch, did not reveal any interference with the peak of TQ. The LOD and LOQ were 3.407 µg/mL and 10.324 µg/mL, respectively. Ten samples of 31.25 µg/mL TQ solution were tested using HPLC technique to check the equipment precision, and the average was 99.5% (RSD = 1.76%). Results showed that the used method is precise due to the low RSD, which was less than 2%. The recovery method's inter- and intra-day repeatability and accuracy were evaluated using 5 concentrations. The findings in Table III demonstrated the method's high repeatability and accuracy.

Entrapment Efficiency and Encapsulation Efficiency

The filtrate was collected upon the synthesis of the TQ-loaded NCs and utilized to perform HPLC-based analysis for the quantification of TQ. The entrapment efficiency (EE %) was 99.6%, and the loading efficiency (LE %) was 25.97%.

Table III Precision and Reproducibility of TQ Analysis and HPLC Method for Assessing Inter- and Intra-day Reproducibility (Mean ± SD, $n = 3$)

	TQ concentration (µg/mL)				
	62.5	31.75	15.625	7.813	3.906
Intra-day % recovery (mean ± SD) ($n = 3$)	98.04 ± 1.64	99.49 ± 1.09	102.28 ± 2.01	99.03 ± 1.68	102.75 ± 0.98
Inter-day % recovery (mean ± SD) ($n = 9$)	96.45 ± 1.98	100.07 ± 1.87	101.56 ± 2.04	100.76 ± 1.88	101.98 ± 1.23

Characterization of the Transdermal Patch

Initial attempts to dry the EVA backing films and the Eudragit second layer in the oven for 5 h at 40 °C resulted in cracked and rough film (P2 and P1, respectively) because of over-drying (see Fig. 7). Therefore, the patches were dried at ambient room temperature (RT) over 2 days. The produced films were transparent, flexible, and easy to peel (P3). However, it separated from the backing layer when casted over it and dried. TQ patches with an EVA backing layer and a layer containing the drug and Eudragit® E were optimized by varying several parameters as depicted in Table I. Increasing the polymer and plasticiser concentrations (P4–P6) produced thick medicated layer that separated from the backing layer upon drying. The addition of 200 µL of aloe vera to the second layer in P7 produced patches that are sticky and could not dry even after 1 week. Therefore, lower Eudragit E100 and aloe vera content and the use of Span 60 as an emulsifying agent were employed (P8). The produced films were transpaernt, flexible, and smooth. Further reudction of Span 60 contnet was examined (P9), and the produced transdermal patch was excellent in terms of flexibility transparency and smoothness. The final patch (P10) was produced using P9 formula with additional content of the TQ/Arg-PA NPs. P10 was dry, clear, flexible, and easy to peel which was used for further characterization techniques. Representative patches are presented in Fig. 7. The selection of Span 60 as nonionic surfactant was based on research findings that Eudragit did not interact with nonionic surfactants [55]. P11 was a replicte of P10 but without aloe vera, which was prepared to be used as a negative control in release and permeation studies.

Thickness, Weight Variation, Drug Content, Folding Endurance, %Solvent Residue, and Moisture Uptake

Table IV displays the thickness, weight uniformity, TQ content uniformity, folding endurance, and solvent residue of a few different Eudragit® patches that have been plasticized using glycerin and aloe vera. The uniformity of the patches' weight, thickness, and drug content suggested that their production process was effective. Different aloe vera concentrations used as penetration enhancers caused variations in folding endurance. The optimal patches according to the results of folding endurance were patches (P9 and

Fig. 7 Representative transdermal patches highlighting the quality of the produced patches
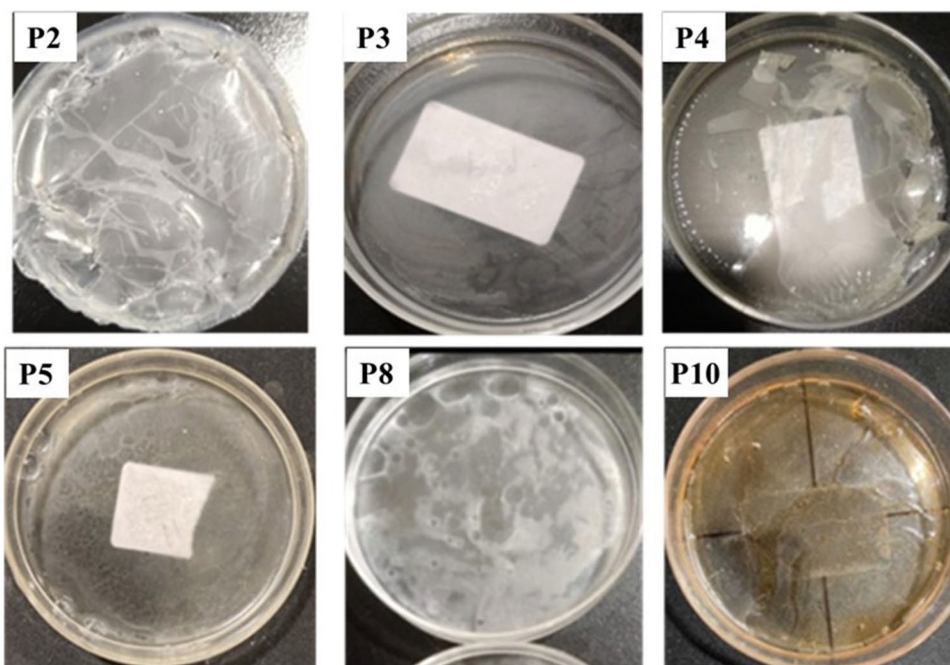
Table IV Properties of Blank and TQ-Loaded Transdermal Patches (Patch Area = 1 cm^2; Mean ± SD; $n = 5$)

Patch	Thickness (mm)	Weight (mg)	Drug content (mg/cm^2) [%]	Folding endurance	%Solvent residue	%Moisture uptake
P6	0.791± 0.56	61.02 ± 2.7	NA	52 ± 7.2	4.86 ± 0.71	4.6 ± 0.32
P8	0.475 ± 0.31	39.96 ± 0.6	NA	233 ± 0.4	7.16 ± 0.61	4.5 ± 0.55
P9	0.422± 0.11	39.02± 0.3	NA	More than 235	6.62 ± 0.74	3.9 ± 0.14
P10	0.475 ± 0.09	49.02 ± 0.7	2.47 ± 0.21 [95.74 ± 8.50]	More than 235	6.46 ± 0.62	4.1 ± 0.11

P10) because patches did not crack, had the best flexibility, and would be able to keep their integrity throughout general application into the skin, according to the folding endurance values, which were adequate. Patch P6 had high polymer concent with no aloe vera or emulsifier, produced cracked films that did not withstand the folding endurance test.

In order to evaluate the integrity of the patches in dry circumstances, solvent residue experiments were carried out. The range of solvent concentration was $4.86 \pm 0.71\%$ and $7.16 \pm 0.61\%$, which demonstrated a asignificant difference (one-way ANOVA, $p = 0.0003$). However, this diference was only between P6 *versus* P8 and P6 *versus* P9 (Tukey post test $p = 0.003$ and 0.0039, respectively), while insignificant among others. This may preserve the patches' structural integrity, lessen their brittleness, and keep their formulas steady over an extended period of storage. However, higher solvent residue content was observed in P8, which contains the highest concentration of emulsifier. However, some water content will maintain the flexibility of the patch and prevent it from becoming brittle, while high moisture content or uptake may affect the quality of the film as well as its microbial burden [56]. Therefore, the properaed patches had an acceptable elevel of moisture content.

To evaluate the stability of the patches under very humid circumstances, moisture absorption experiments were conducted. When the samples were kept at 100% RH, all patches showed low moisture absorption rate and water uptake, but this low water uptake affects the bi-layer system by separating the two layers from each other. As a result, all patches must be kept at room temperature because the produced transdermal patches were affected by highly humid conditions. The low moisture uptake of the films could be attributed to the hydrophobic nature of Eudragit E100 [57, 58]. Upon compasirion, there was no statistically significant difference bwtween formulations in terms of moisture uptake (one-way ANOVA, $p = 0.0951$). The key component is Eugragit E100, and it is a hydrophobic polymer, and therefore, water uptake was not high.

Stability of the Transdermal Patch

The final produced patches (P10) were stored at 4 °C, 25 °C, and 40 °C. The patches' morphology changed after 3 months, according to a visual evaluation. Furthermore, there were significant differences in the thickness, weight, and absolute medication content of each patch. All the patches that were placed in the oven at 40 °C melted and became liquid which confirms that the patches were temperature sensitive. While patches that were kept in the refrigerator at 4 °C became rigid and had rough surfaces, it was not easy to peel and crack. As a result, the optimum temperature to store this transdermal patch is room temperature (25 °C). (Table V summarizes the findings).

Table V Properties of TQ Transdermal Patches (P10) Stored at Different Temperatures for 3 Months

Physical state	4 °C Rigid	25 °C Dry but not rigid	40 °C Melt
Cracked and breakable	✓	✗	✗
Mixed layers	✗	✗	✓
Smooth	✗	✓	✗
Rough surface	✓	✗	✗
Easy to peel and use	✗	✓	✗
Flexible	✗	✓	✗
Transparent	✗	✓	✓

Drug Release and Permeation Studies

A good candidate drug for transdermal drug delivery is a drug with a molecular weight ˂ 500 Da, a melting point ˂ 200 °C, an aqueous solubility ˂ 1 mg/mL, and a partition coefficient between 1 and 4 [59]. Therefore, TQ is a potential candidate for transdermal drug delivery owing to its low molecular weight of 164.2 Da, melting point of around 47 °C, low aqueous solubility of 1–1.8 mg/mL, and partition coefficient of 1.7 [7, 46]. The next set of investigations focused on the TQ's *in vitro* release and permeation profiles (Fig. 8). The release profile as depicted in Fig. 8a revealed the sustained release of TQ from the transdermal patches. Upon comparison, the release of TQ from aloe vera-containing patches demonstrated higher release at each data point; however, the difference is not significant ($p > 0.05$). The release kinetics of TQ was modeled, and the results are summarized in Table VI. From the table, the release profile of TQ from P10 and P11 patches followed the Higuchi model (R^2 of 0.9839 and 0.9846, respectively), suggesting that the release of the drug from the transdermal patches was dominated by the diffusion mechanism [56, 60]. However, for a better understanding of the diffusion pattern and whether it is Fickian or non-Fickian diffusion, the Korsmeyer -Peppas model was used. The results showed a high correlation ($R^2 = 0.9825$ and 0.9822 for P10 and P11, respectively), where the release pattern is governed by the value of "n." If the n value was above 1, this implies supercase transport, which represents macromolecular relaxation of the polymeric chains [7]. It is expected as the transdermal patches are made of a polymeric material and the TQ-loaded nanoaggregates are also included in another polymeric material. Such barriers can support the non-Fickian diffusion profile. The extended-release profile of TQ is expected to mitigate the irritant effect of TQ.

The permeation of TQ through the transdermal patches and STRAT-M® membrane over time was determined (Fig. 8b). After 24 h, almost 775.38 ± 62.03 $\mu g/cm^2$ and 588.27 ± 83.74 $\mu g/cm^2$ of P10 and P11, respectively, were
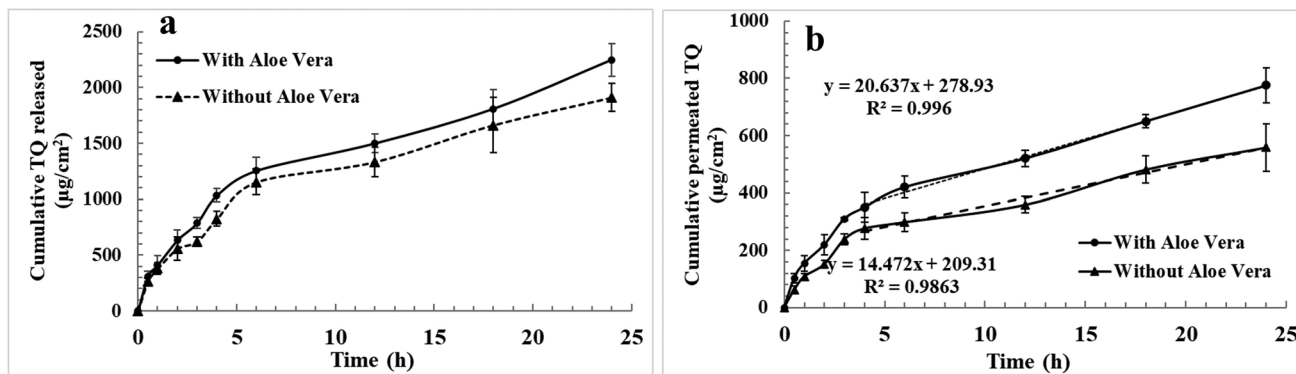
Fig. 8 **a** *In vitro* release profile of TQ from the transdermal patches (with and without aloe vera P10 and P11, respectively) in phosphate buffer (pH 6.8). **b** *In vitro* permeation profile of TQ from the trans- dermal patches (with and without aloe vera P10 and P11, respectively) through STRAT M® membrane in phosphate buffer (pH 6.8) (mean ± SD, n = 3)

Table VI Summary of the Modeling the Release Profiles of P10 and P11 Parameters (Constant, Coefficient of Determination (R^2), and the "n" Value) for Each Mathematical Model

Mathematical model	P10 patch with aloe vera			P11 patch without aloe vera		
	R^2	Constant	n	R^2	Constant	N
Zero order	0.9302	75.47	-	0.9261	66.828	-
First order	0.9426	211.00	-	0.9411	187.1038	
Higuchi model	0.9839	442.50	-	0.9846	392.84	
Hixon Crowell model	0.9690	0.2382	-	0.9678	0.1829	
Korsmeyer-Peppas model	0.9825	172.89	1.842	0.9822	171.333	1.8844

released. A sustained release pattern was observed over 24 h. It is worth mentioning that Eudragit E100 would dissolve at a pH below 5 [61]. The average healthy adult skin pH is within the range of 5.6 ± 0.5, while it will be lower with psoriasis patients (5.2 ± 0.5) [62]. Therefore, it is expected that Eudragit E100 will have better solubility, which will favor the release profile of TQ [59]. The flux value of TQ from aloe vera-containing transdermal patch (P10) was higher than that of a transdermal patch without aloe vera (P11), with values of 20.64 and 14.47 $\mu g/cm^2$ h, respectively. The presence of aloe vera enhanced the flux by 42.64%. Therefore, the use of aloe vera contributed to enhancing the permeation of TQ through the membrane. It is worth mentioning that aloe vera contributed to the increase in permeation rather than the enhancement of the release of TQ from the patches.

Conclusions

This study demonstrated the potential of nanostructured L-arginine-based polyamide (Arg-PA) embedded in bi-layered transdermal patches to enhance the skin delivery of thymoquinone. The TQ-Arg-PA was produced by an interfacial polycondensation technique. Nanoaggregates with

a high percentage of EE (99.6%) and LE (25.97%) and good colloidal stability in terms of size, surface charge, and particle distribution were obtained. The release of thymoquinone was extended after incorporation into the Arg-PA, which could have helped mitigate thymoquinone's slight irritant effect. The TQ-Arg-PA nanocapsules were incorporated into transdermal patches containing EVA, Eudragit E100, glycerin, Span 60, and aloe vera—as penetration enhancer. The patches containing aloe vera provided good penetration enhancement with an increase in thymoquinone flux (Jss) of 42.64%. Therefore, the results suggest that transdermal delivery of TQ could be a promising approach for optimal targeting for skin conditions such as psoriasis, as well as for reducing systemic exposure. However, clinical studies need to be carried out to assess its suitability in clinical practice for the management of psoriasis and other skin conditions.

Data Availability All data generated or analyzed during this study are included in this published article.

Declarations

Conflict of Interest The authors declare no competing interests.

References

1. Badıllı U, Şen T, Tarımcı N. Microparticulate based topical delivery system of clobetasol propionate. AAPS PharmSciTech. 2011;12(3):949–57.

2. Vaillant L, Berson M, Machet L, Callens A, Pourcelot L, Lorette G. Ultrasound imaging of psoriatic skin: A noninvasive technique to evaluate treatment of psoriasis. Int J Dermatol. 1994;33(11):786–90.

3. Bailey EE, Ference EH, Alikhan A, Hession MT, Armstrong AW. Combination treatments for psoriasis: A systematic review and meta-analysis. Arch Dermatol. 2012;148(4):511–22.

4. Kaur A, Katiyar SS, Kushwah V, Jain S. Nanoemulsion loaded gel for topical co-delivery of clobitasol propionate and calcipotriol in psoriasis. Nanomed Nanotechnol Biol Med. 2017;13(4):1473–82.

5. Ali MY, Akter Z, Mei Z, Zheng M, Tania M, Khan MA. Thymoquinone in autoimmune diseases: Therapeutic potential and molecular mechanisms. Biomed Pharmacother. 2020;2021(134):111157.

6. Khatoon K, Ali A, Ahmad FJ, Hafeez Z, Rizvi MMA, Akhter S, et al. Novel nanoemulsion gel containing triple natural bio-actives combination of curcumin, thymoquinone, and resveratrol improves psoriasis therapy: In vitro and in vivo studies. Drug Deliv Transl Res. 2020;11(3):1245–60.

7. Dahmash EZ, Ali DK, Alyami HS, Abdulkarim H, Alyami MH, Aodah AH. Novel Thymoquinone nanoparticles using poly(Ester Amide) Based on L-Arginine-Targeting pulmonary drug delivery. Polymers (Basel). 2022;14(6):1082.

8. Gholamnezhad Z, Havakhah S, Boskabady MH. Preclinical and clinical effects of Nigella sativa and its constituent, thymoquinone: A review. Vol. 190, Journal of Ethnopharmacology. Elsevier; 2016. p. 372–386.

9. Alotaibi FO, Mustafa G, Ahuja A. Study of enhanced anti-inflammatory potential of nigella sativa in topical nanoformulation. Int J Pharm Pharm Sci. 2018;10(7):41.

10 Eid AM, Elmarzugi NA, Abu Ayyash LM, Sawafta MN, Daana HI. A review on the cosmeceutical and external applications of Nigella sativa. J Trop Med. 2017;2017:1–6.

11 Saka R, Chella N. Nanotechnology for delivery of natural therapeutic substances: A review. Environ Chem Lett. 2020;19:1097–106.

12. Tabassum S, Rosli N, Ichwan SJA, Mishra P. Thymoquinone and its pharmacological perspective: A review. Pharmacol Res Chinese Med. 2021;1:100020.

13. Sallehuddin N, Nordin A, Idrus RBH, Fauzi MB. Nigella sativa and its active compound, thymoquinone, accelerate wound healing in an in vivo animal model: A comprehensive review. Int J Environ Res Public Health. 2020;17(11):1–17.

14. Badary OA, Al-Shabanah OA, Nagi MN, Al-Bekairi AM, Elmazar MMA. Acute and subchronic toxicity of thymoquinone in mice. Drug Dev Res. 1998;44(2–3):56–61.

15. Ali A, Ali S, Aqil M, Imam SS, Ahad A, Qadir A. Thymoquinone loaded dermal lipid nano particles: Box Behnken design optimization to preclinical psoriasis assessment. J Drug Deliv Sci Technol [Internet]. 2019;52:713–21. Available from: https://doi.org/10.1016/j.jddst.2019.05.041.

16. Rosso A, Zuccaro S. Determination of alkaloids from the colchicine family by reversed-phase high-performance liquid chromatography. J Chromatogr A. 1998;825(1):96–101.

17. Sharma K, Mittal A, Chauhan N. Aloe vera as penetration enhancer. Int J Drug Dev Res. 2015;7(1):31–43.

18. Radha MH, Laxmipriya NP. Evaluation of biological properties and clinical effectiveness of aloe vera: A systematic review. J Tradit Complement Med. 2015;5(1):21–6.

19. Vashisth I, Ahad A, Aqil M, Agarwal SP. Investigating the potential of essential oils as penetration enhancer for transdermal losartan delivery: Effectiveness and mechanism of action. Asian J Pharm Sci. 2014;9(5):260–7.

20. Kesarwani A, Yadav AK, Singh S, Gautam H, Singh HN, Sharma A, et al. An official publication of association of pharmacy professionals theoretical aspects of transdermal drug delivery system. Bull Pharm Res. 2013;3(2):78–89.

21 Neupane R, Boddu SHS, Renukuntla J, Babu RJ, Tiwari AK. Alternatives to biological skin in permeation studies: Current trends and possibilities. Pharmaceutics. 2020;12(2):152.

22. Rajan R, Sheba Rani ND, Kajal G, Sanjoy Kumar D, Jasmina K, Arunabha N. Design and in vitro evaluation of chlorpheniramine maleate from different Eudragit based matrix patches: Effect of platicizer and chemical enhancers. Ars Pharm. 2009;50(4):177–94.

23. Nampoothiri V, Sudhir AS, Joseph M V, Mohamed Z, Menon V, Charani E, et al. Mapping the implementation of a clinical pharmacist-driven antimicrobial stewardship programme at a tertiary care centre in South India. Vol. 10, Antibiotics. 2021.

24. Li C, Wang M, Liu Z, Xu Y, Zhou C, Wang L. Kaolinite-armoured polyurea microcapsules fabricated on Pickering emulsion: Controllable encapsulation and release performance of a lipophilic compound. Clay Miner. 2021;56(1):46–54.

25. Negi P, Sharma I, Hemrajani C, Rathore C, Bisht A, Raza K, et al. Thymoquinone-loaded lipid vesicles: A promising nanomedicine for psoriasis. BMC Complement Altern Med [Internet]. 2019;19(1):334. Available from: https://doi.org/10.1186/s12906-019-2675-5.

26. Bruno MC, Gagliardi A, Mancuso A, Barone A, Tarsitano M, Cosco D, et al. Oleic acid-based vesicular nanocarriers for topical delivery of the natural drug thymoquinone: Improvement of anti-inflammatory activity. J Control Release [Internet]. 2022;352:74–86. Available from: https://www.sciencedirect.com/science/article/pii/S0168365922006812. Accessed 18 Nov 2023.

27. Odeh F, Ismail SI, Abu-Dahab R, Mahmoud IS, Al BA. Thymoquinone in liposomes: A study of loading efficiency and biological activity towards breast cancer. Drug Deliv. 2012;19(8):371–7.

28. Mansour MA, Nagi MN, El-Khatib AS, Al-Bekairi AM. Effects of thymoquinone on antioxidant enzyme activities, lipid peroxidation and DT-diaphorase in different tissues of mice: A

possible mechanism of action. Cell Biochem Funct [Internet]. 2002;20(2):143–51. Available from: https://doi.org/10.1002/cbf.968.

29. Singh N, Joshi A, Toor AP, Verma G. Drug delivery: Advancements and challenges [Internet]. Nanostructures for Drug Delivery. Elsevier Inc.; 2017. 865–886 p. Available from: https://doi.org/10.1016/B978-0-323-46143-6.00027-0.

30. Brady J, Dürig T, Lee PI, Li J-X. Chapter 7 - Polymer properties and characterization. In: Qiu Y, Chen Y, Zhang GGZ, Yu L, Mantri RVBT-DSODF (Second E, editors. Boston: Academic Press; 2017. p. 181–223.

31. Gavasane AJ, Pawar HA. Synthetic biodegradable polymers used in controlled drug delivery system: An overview. Clin Pharmacol Biopharm. 2014;3(2):1–7.

32. Khan W, Muthupandian S, Farah S, Kumar N, Domb AJ. Biodegradable polymers derived from amino acids. Macromol Biosci. 2011;11(12):1625–36.

33. He P, Liu H, Tang Z, Deng M, Yang Y, Pang X, et al. Poly(ester amide) blend microspheres for oral insulin delivery. Int J Pharm. 2013;455(1–2):259–66.

34. Pang X, Wu J, Reinhart-King C, Chu CC. Synthesis and characterization of functionalized water soluble cationic poly(ester amide)s. J Polym Sci Part A Polym Chem. 2010;48(17):3758–66.

35. Zhang S, Xin P, Ou Q, Hollett G, Gu Z, Wu J. Poly (ester amide)-based hybrid hydrogels for efficient transdermal insulin delivery. J Mater Chem B [Internet]. 2018;6(42):6723–30. Available from: https://doi.org/10.1039/C8TB01466C.

36. Alyami HS, Ali DK, Jarrar Q, Jaradat A, Aburass H, Mohammed AA, et al. Taste masking of promethazine hydrochloride using l-arginine polyamide-based nanocapsules. Molecules [Internet]. 2023;28(2). Available from: https://www.mdpi.com/1420-3049/28/2/748. Accessed 12 Nov 2023.

37. Wu J, Mutschler MA, Chu CC. Synthesis and characterization of ionic charged water soluble arginine-based poly(ester amide). J Mater Sci Mater Med. 2011;22(3):469–79.

38. Zhou Y, Han S, Liang Z, Zhao M, Liu G, Wu J. Progress in arginine-based gene delivery systems. J Mater Chem B. 2020;8(26):5564–77.

39. Zhou Y, Liu G, Huang H, Wu J. Advances and impact of arginine-based materials in wound healing. J Mater Chem B. 2021;9(34):6738–50.

40. Felton LA. Mechanisms of polymeric film formation. Int J Pharm. 2013;457(2):423–7.

41. Fonseca AC, Coelho JFJ, Valente JFA, Correia TR, Correia IJ, Gil MH, et al. Poly(ester amide)s based on (L)-lactic acid oligomers and α-amino acids: Influence of the α-amino acid side chain in the poly(ester amide)s properties. J Biomater Sci Polym Ed. 2013;24(12):1391–409.

42. Fonseca AC, Coelho JFJ, Gil MH, Simões PN. Poly(ester amide)s based on l-lactic acid oligomers and glycine: The role of the central unit of the l-lactic acid oligomers and their molecular weight in the poly(ester amide)s properties. Polym Bull. 2014;71(12):3085–109.

43. Song Y, Fan JB, Wang S. Recent progress in interfacial polymerization. Mater Chem Front. 2017;1(6):1028–40.

44. Assaf SM, Alarabi Sallam AS, Ghanem AM. Design and evaluation of transdermal delivery system containing tamsulosin hydrochloride. J Drug Deliv Sci Technol. 2019;51:524–34.

45. ICH. Validation of analytical procedures: Text and methodology Q2(R1). Int Conf Harmon Tech Requir Regist Pharm Hum Use. 2005;4.

46. Chemeo. Chemical properties of Thymoquinone [Internet]. 2023 [cited 2023 Dec 8]. Available from: https://www.chemeo.com/cid/85-850-4/Thymoquinone.

47. Dash S, Murthy PN, Nath L, Chowdhury P. Kinetic modeling on drug release from controlled drug delivery systems. Acta Pol Pharm. 2010;67(3):217–23.

48. Rani R, Dahiya S, Dhingra D, Dilbaghi N, Kim K-H, Kumar S. Improvement of antihyperglycemic activity of nano-thymoquinone in rat model of type-2 diabetes. Chem Biol Interact. 2018;295:119–32.

49. Alyami MH, Dahmash EZ, Ali DK, Alyami HS, AbdulKarim H, Alsudir SA. Novel fluticasone propionate and salmeterol fixed-dose combination nano-encapsulated particles using polyamide Based on L-lysine. Pharmaceuticals. 2022;15(3):321.

50. AbdulKarim H, Ali DK, Taybeh E, Alyami HS, Assaf SM, Dahmash EZ. Novel poly (ester amide) derived from tyrosine amino acid for targeted pulmonary drug delivery of fluticasone propionate. J Appl Polym Sci. 2023;140:e53672.

51. Alam S, Khan ZI, Mustafa G, Kumar M, Islam F, Bhatnagar A, et al. Development and evaluation of thymoquinone-encapsulated chitosan nanoparticles for nose-to-brain targeting: A pharmacoscintigraphic study. Int J Nanomedicine [Internet]. 2012/11/09. 2012;7:5705–18. Available from: https://pubmed.ncbi.nlm.nih.gov/23180965.

52. Pant A, Negi JS. Novel controlled ionic gelation strategy for chitosan nanoparticles preparation using TPP-β-CD inclusion complex. Eur J Pharm Sci. 2018;112(1):180–5.

53. Chen D, Liu T, Kang J, Xu R, Cao Y, Xiang M. Enhancing the permeability and antifouling properties of polyamide composite reverse osmosis membrane by surface modification with zwitterionic amino acid l-arginine. Adv Mater Interfaces. 2019;6(14):1900706.

54. Hu S, Sun L, Liu M, Zhu H, Guo H, Sun H, et al. A highly dispersible silica pH nanosensor with expanded measurement ranges. New J Chem. 2015;39(6):4568–74.

55. Ofridam F, Lebaz N, Gagnière É, Mangin D, Elaissari A. Polymethylmethacrylate derivatives Eudragit E100 and L100: Interactions and complexation with surfactants. Polym Adv Technol [Internet]. 2021;32(1):379–90. Available from: https://onlinelibrary.wiley.com/doi/abs/10.1002/pat.5093.

56. Ubaidulla U, Reddy MVS, Ruckmani K, Ahmad FJ, Khar RK. Transdermal therapeutic system of carvedilol: Effect of hydrophilic and hydrophobic matrix on in vitro and in vivo characteristics. Aaps Pharmscitech. 2007;8(1):2.

57. Doerdelmann G, Kozlova D, Epple M. A pH-sensitive poly (methyl methacrylate) copolymer for efficient drug and gene delivery across the cell membrane. J Mater Chem B. 2014;2(41):7123–31.

58 Sawant PD, Luu D, Ye R, Buchta R. Drug release from hydroethanolic gels. Effect of drug's lipophilicity (log P), polymer–drug interactions and solvent lipophilicity. Int J Pharm. 2010;396(1–2):45–52.

59. Damgalı Ş, Özdemir S, Kaya G, Demirkoz AB, Üner M. Development of monolithic matrix type transdermal patches containing cinnarizine: Physical characterization and permeation studies. Brazilian J Pharm Sci. 2022;58:e19859. https://doi.org/10.1590/s2175-97902022e19859.

60. Wójcik-Pastuszka D, Krzak J, Macikowski B, Berkowski R, Osiński B, Musiał W. Evaluation of the release kinetics of a pharmacologically active substance from model intra-articular implants replacing the cruciate ligaments of the knee. Materials (Basel). 2019;12(8):1202.

61. Sester C, Ofridam F, Lebaz N, Gagnière E, Mangin D, Elaissari A. pH-Sensitive methacrylic acid–methyl methacrylate copolymer Eudragit L100 and dimethylaminoethyl methacrylate, butyl methacrylate, and methyl methacrylate tri-copolymer Eudragit E100. Polym Adv Technol [Internet]. 2020;31(3):440–50. Available from: https://onlinelibrary.wiley.com/doi/abs/10.1002/pat.4780.

62 Bigliardi PL. Role of skin pH in psoriasis. pH Ski Issues Challenges. 2018;54:108–14.